arXiv:1604.08526v2 [hep-ph] 18 Aug 2016

Polarized 3 parton production in inclusive DIS at small x

Alejandro Ayala[1,2], Martin Hentschinski[1,3], Jamal Jalilian-Marian[4,5], Maria Elena Tejeda-Yeomans[6]

[1]Instituto de Ciencias Nucleares, Universidad Nacional Autónoma de México, Apartado Postal 70-543, Ciudad de México 04510, Mexico
[2]Centre for Theoretical and Mathematical Physics, and Department of Physics, University of Cape Town, Rondebosch 7700, South Africa
[3]Facultad de Ciencias Físico Matemáticas, Benemérita Universidad Autónoma de Puebla, Puebla 1152, Mexico
[4]Department of Natural Sciences, Baruch College, CUNY, 17 Lexington Avenue, New York, NY 10010, USA
[5]CUNY Graduate Center, 365 Fifth Avenue, New York, NY 10016, USA
[6]Departamento de Física, Universidad de Sonora, Boulevard Luis Encinas J. y Rosales, Colonia Centro, Hermosillo, Sonora 83000, Mexico

Abstract

Azimuthal angular correlations between produced hadrons/jets in high energy collisions are a sensitive probe of the dynamics of QCD at small x. Here we derive the triple differential cross section for inclusive production of 3 polarized partons in DIS at small x. The target proton or nucleus is described using the Color Glass Condensate (CGC) formalism. The resulting expressions are used to study azimuthal angular correlations between produced partons in order to probe the gluon structure of the target hadron or nucleus. Our analytic expressions can also be used to calculate the real part of the Next to Leading Order (NLO) corrections to di-hadron production in DIS by integrating out one of the three final state partons.

Gluon saturation in QCD at small Bjorken x was proposed by Gribov, Levin and Ryskin as a dynamical mechanism by which perturbative unitarity of QCD cross sections at high energy (small x) is restored [1]. McLerran and Venugopalan [2] formulated an effective action approach to gluon saturation which describes a high energy hadron or nucleus as a Color Glass Condensate (CGC); a state of high occupancy number which is a weakly-coupled yet non-perturbative system of gluons characterized by a semi-hard scale Q_s, called the saturation scale. This is a systematic approach which allows to apply semi-classical methods to particle production in high energy hadronic collisions. While there is a large body of evidence pointing to the importance of saturation physics in the small x regime of high energy collisions [3], more studies are needed to constrain the parameters of the approach and to clarify further its kinematic limits.

The bulk of current studies of Deep Inelastic Scattering (DIS) of electrons on a target proton or nucleus [4, 5] concentrates on inclusive observables, such as (diffractive) structure

functions F_2 and F_L, which provide access to 2-point correlations (of Wilson lines) in the target as encoded in the extracted color dipole factors. Dynamics of gluon saturation is however far richer than that contained in 2-point functions: observables in the CGC approach are given in terms of multi-point correlators of Wilson lines, the most prominent one being the Quadrupole – the 4-point correlation function of Wilson lines which appears in multi-parton production processes in DIS and pA collisions [6]. These higher point correlators carry much more information about the dynamics of gluon saturation than dipoles. However, unlike the dipoles, higher point correlators are experimentally not well-constrained. To access them experimentally, it is needed to study observables with multi-particle final states in a clean experimental environment such as DIS. A first example is azimuthal angular correlation of two hadrons [7] which provides access to the 4-point correlation function and constitutes a key process in saturation searches at future Electron Ion Colliders, see *e.g.* [8].

In this Letter we propose to use azimuthal angular correlations of 3 partons in inclusive DIS to explore the dynamics of saturated partonic matter. The novel feature of this process is that, since it involves two relative angles between the three produced partons, it offers an additional handle compared to di-hadron azimuthal angular correlations, which involve only one relative angle. Moreover, unlike 2 parton production, the 3 parton cross-section depends non-linearly on both quadrupoles and dipoles and allows therefore to access different aspects of those correlators; it therefore acts also as a complementary tool for their exploration.

In the following we present our results for the triple differential cross section for inclusive production of three partons in DIS. Our expression keeps the full helicity dependence of initial and final state particles and therefore can be used in principle to study fragmentation of polarized partons into hadrons [9]. In order to exhibit the effect of gluon saturation on azimuthal angular correlations, we perform a first study of the angular structure of the three produced partons for a particular angular configuration, in the transverse momentum region just above the saturation scale. This allows us to work in the dilute limit of the CGC, but still exhibits the main features of the saturation dynamics. We find that saturation effects reduce the magnitude of the correlation peak while simultaneously widening it. We further stress that our analytic expressions can be used to compute the real contributions to the Next to Leading Order (NLO) corrections [10] to inclusive di-hadron production in DIS [8].

We consider the process depicted in Fig. 1

$$\gamma^*(l) + \text{target}\,(P) \to q(p) + \bar{q}(q) + g(k) + X, \tag{1}$$

with photon virtuality $l^2 = -Q^2$. The target is a high energy hadron/nucleus, represented by a strong background color field (shock wave) $A^\mu \sim 1/g$ in light-cone gauge $A \cdot n = 0$ with $A^+(x^-, x_t) = \delta(x^-)\alpha(x_t)$. Light-cone vectors $n, \bar{n}$ are defined through the four momenta of virtual photon and target, *i.e.* $n \sim P$ and $n \cdot \bar{n} = 1$ with $v^- \equiv n \cdot v$ for a generic four vector v. Amplitudes are written in terms of momentum space quark and gluon propagators in the presence of the background field

$$S_{F,il}(p,q) \equiv S^{(0)}_{F,ij}(p)\,\tau_{F,jk}(p,q)\,S^{(0)}_{kl}(q), \qquad G^{ad}_{\mu\nu}(p,q) \equiv G^{(0),ab}_{\mu\lambda}(p)\,\tau^{bc}_{g}(p,q)\,G^{(0),cd,\lambda}_{\nu}(q) \tag{2}$$

with the conventional free fermion and gluon propagator, $S^{(0)}_{F,ij}(p) = i\delta_{ij}/(\not{p} + i\epsilon)$ and $G^{(0),ab}_{\mu\nu} = i\delta^{ab}d_{\mu\nu}(k)/(k^2 + i\epsilon)$ respectively, and $d_{\mu\nu}(k) = [-g_{\mu\nu} + (k_\mu n_\nu + k_\nu n_\mu)/n \cdot k]$ the light-cone

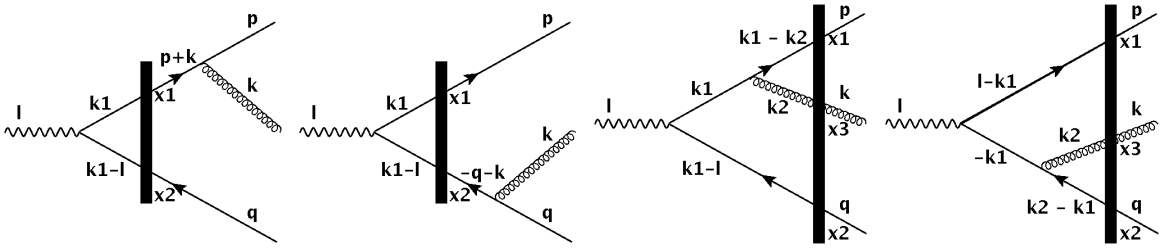

Figure 1: 3-parton production diagrams. The solid thick line represents interactions with the target (shock wave). The arrows indicate the direction of fermion charge flow. The photon momentum is incoming whereas all the final state momenta are outgoing.

gauge polarization tensor. Furthermore

$$\tau_{F,ij}(p,q) \equiv (2\pi)\delta(p^- - q^-)\not{p}\int d^2x_t\; e^{i(p_t-q_t)\cdot x_t}\left[\theta(p^-)V_{ij}(x_t) - \theta(-p^-)V^\dagger_{ij}(x_t)\right],$$
$$\tau_g^{ab}(p,q) \equiv -4\pi p^-\delta(p^- - q^-)\int d^2x_t\; e^{i(p_t-q_t)\cdot x_t}\left[\theta(p^-)U^{ab}(x_t) - \theta(-p^-)(U^\dagger)^{ab}(x_t)\right]], \quad (3)$$

where $U^{ba}(z_t) = 2\mathrm{tr}(t^a V(z_t) t^b V^\dagger(z_t))$ and

$$V(x_t) \equiv \hat{P}\exp\{ig\int_{-\infty}^{\infty} dx^- A_a^+(x^-, x_t)\, t_a\}, \quad (4)$$

the fundamental SU(N_c) Wilson line. The four matrix elements corresponding to Fig. 1 read

$$i\mathcal{A}_1 = (ie)(ig)\int \frac{d^4k_1}{(2\pi)^4}\bar{u}(p)\gamma^\mu t^a S_F(p+k,k_1)\gamma^\nu S_F(k_1-l,-q)\left[S_F^{(0)}(-q)\right]^{-1} v(q)\,\epsilon_\nu(l)\,\epsilon^*_\mu(k),$$
$$i\mathcal{A}_2 = (ie)(ig)\int \frac{d^4k_1}{(2\pi)^4}\bar{u}(p)\left[S_F^{(0)}(p)\right]^{-1} S_F(p,k_1)\,\gamma^\nu S_F(k_1-l,-q-k)\,\gamma^\mu t^a\, v(q)\,,\epsilon_\nu(l)\,\epsilon^*_\mu(k)$$
$$i\mathcal{A}_3 = (ie)(ig)\int \frac{d^4k_1}{(2\pi)^4}\int \frac{d^4k_2}{(2\pi)^4}\bar{u}(p)\left[S_F^{(0)}(p)\right]^{-1} S_F(p,k_1-k_2)\gamma^\lambda t^c\, S_F^{(0)}(k_1)\gamma^\nu$$
$$S_F(k_1-l,-q)\left[S_F^{(0)}(-q)\right]^{-1} v(q)\left[G_\lambda^{\ \delta}\right]^{ca}(k_2,k)\left[G_\delta^{(0),\mu}(k)\right]^{-1}\epsilon_\nu(l)\epsilon^*_\mu(k),$$
$$i\mathcal{A}_4 = (ie)(ig)\int \frac{d^4k_1}{(2\pi)^4}\int \frac{d^4k_2}{(2\pi)^4}\bar{u}(p)\left[S_F^{(0)}(p)\right]^{-1} S_F(p,l-k_1)\,\gamma^\nu\, S_F^{(0)}(-k_1)\gamma^\lambda t^c$$
$$S_F(k_2-k_1,-q)\left[S_F^{(0)}(-q)\right]^{-1}\left[G_\lambda^{\ \delta}\right]^{ca}(k_2,k)\left[G_\delta^{(0)\mu}(k)\right]^{-1}\epsilon_\nu(l)\,\epsilon^*_\mu(k), \quad (5)$$

where $\epsilon_\nu(l), \epsilon^*_\mu(k)$ denote polarization vectors of the incoming virtual photon and the outgoing gluon respectively. With flux factor $\mathcal{F} = 2l^-$, photon momentum fractions $\{z_1, z_2, z_3\} = \{p^-/l^-, q^-/l^-, k^-/l^-\}$ and the three-particle phase space

$$d\Phi^{(3)} = \frac{1}{(2\pi)^8}\, d^4p\, d^4q\, d^4k\,\delta(p^2)\delta(q^2)\delta(k^2)\delta(l^- - p^- - k^- - q^-)$$
$$= 2l^-\frac{d^2p_t\, d^2q_t\, d^2k_t}{(64\pi^4 l^-)^2}\frac{dz_1\, dz_2\, dz_3}{z_1\, z_2\, z_3}\delta(1-\sum_{i=1}^{3} z_i) \quad (6)$$

the differential 3-parton production cross-section reads

$$d\sigma = \frac{1}{\mathcal{F}} \left\langle |\mathcal{A}(A^+) - \mathcal{A}(0)|^2 \right\rangle_{A^+} d\Phi^{(3)}, \tag{7}$$

where $\langle \ldots \rangle_{A_+}$ denotes the average over background field configurations. The differential cross-section can be expressed in terms of 6 leading N_c terms and one N_c suppressed term. With dipole and quadrupole given by

$$S^{(2)}_{(\boldsymbol{x}_1\boldsymbol{x}_2)} \equiv \frac{1}{N_c}\mathrm{tr}\left[V(\boldsymbol{x}_1)V^\dagger(\boldsymbol{x}_2)\right], \quad S^{(4)}_{(\boldsymbol{x}_1\boldsymbol{x}_2\boldsymbol{x}_3\boldsymbol{x}_4)} \equiv \frac{1}{N_c}\mathrm{tr}\left[V(\boldsymbol{x}_1)V^\dagger(\boldsymbol{x}_2)V(\boldsymbol{x}_3)V^\dagger(\boldsymbol{x}_4)\right], \tag{8}$$

we find the following set of operators,

$$\begin{aligned}
N^{(4)}(\boldsymbol{x}_1,\boldsymbol{x}_2,\boldsymbol{x}_3,\boldsymbol{x}_4) &\equiv 1 + S^{(4)}_{(\boldsymbol{x}_1\boldsymbol{x}_2\boldsymbol{x}_3\boldsymbol{x}_4)} - S^{(2)}_{(\boldsymbol{x}_1\boldsymbol{x}_2)} - S^{(2)}_{(\boldsymbol{x}_3\boldsymbol{x}_4)}\,, \\
N^{(22)}(\boldsymbol{x}_1,\boldsymbol{x}_2|\boldsymbol{x}_3,\boldsymbol{x}_4) &\equiv \left[S^{(2)}_{(\boldsymbol{x}_1\boldsymbol{x}_2)} - 1\right]\left[S^{(2)}_{(\boldsymbol{x}_3\boldsymbol{x}_4)} - 1\right] \\
N^{(24)}(\boldsymbol{x}_1,\boldsymbol{x}_2|\boldsymbol{x}_3,\boldsymbol{x}_4,\boldsymbol{x}_5,\boldsymbol{x}_6) &\equiv 1 + S^{(2)}_{(\boldsymbol{x}_1\boldsymbol{x}_2)}S^{(4)}_{(\boldsymbol{x}_3\boldsymbol{x}_4\boldsymbol{x}_5\boldsymbol{x}_6)} - S^{(2)}_{(\boldsymbol{x}_1\boldsymbol{x}_2)}S^{(2)}_{(\boldsymbol{x}_3\boldsymbol{x}_6)} - S^{(2)}_{(\boldsymbol{x}_4\boldsymbol{x}_5)}\,, \\
N^{(44)}(\boldsymbol{x}_1,\boldsymbol{x}_2,\boldsymbol{x}_3,\boldsymbol{x}_4|\boldsymbol{x}_5,\boldsymbol{x}_6,\boldsymbol{x}_7,\boldsymbol{x}_8) &\equiv 1 + S^{(4)}_{(\boldsymbol{x}_1\boldsymbol{x}_2\boldsymbol{x}_3\boldsymbol{x}_4)}S^{(4)}_{(\boldsymbol{x}_5\boldsymbol{x}_6\boldsymbol{x}_7\boldsymbol{x}_8)} - S^{(2)}_{(\boldsymbol{x}_1\boldsymbol{x}_4)}S^{(2)}_{(\boldsymbol{x}_5\boldsymbol{x}_8)} \\
&\quad - S^{(2)}_{(\boldsymbol{x}_2\boldsymbol{x}_3)}S^{(2)}_{(\boldsymbol{x}_6\boldsymbol{x}_7)}.
\end{aligned} \tag{9}$$

For diffractive reactions, corresponding to color singlet exchange between the $q, \bar{q}, g$ state and target, all of the above quadrupoles are found to factorize into the product of two dipoles, $S^{(4)}_{(\boldsymbol{x}_i\boldsymbol{x}_j\boldsymbol{x}_k\boldsymbol{x}_l)} \to S^{(2)}_{(\boldsymbol{x}_i\boldsymbol{x}_l)}S^{(2)}_{(\boldsymbol{x}_j\boldsymbol{x}_k)}$. With α_{em} and α_s the electromagnetic and strong coupling constants, and e_f the electro-magnetic charge of the quark with flavor f we obtain the following leading N_c result:

$$\begin{aligned}
&\frac{d\sigma^{T,L}}{d^2\boldsymbol{p}\,d^2\boldsymbol{k}\,d^2\boldsymbol{q}\,dz_1dz_2} = \\
&= \frac{\alpha_s\alpha_{em}e_f^2N_c^2}{z_1z_2z_3(2\pi)^2}\prod_{i=1}^{3}\prod_{j=1}^{3}\int\frac{d^2\boldsymbol{x}_i}{(2\pi)^2}\int\frac{d^2\boldsymbol{x}'_j}{(2\pi)^2}e^{i\boldsymbol{p}(\boldsymbol{x}_1-\boldsymbol{x}'_1)+i\boldsymbol{q}(\boldsymbol{x}_2-\boldsymbol{x}'_2)+i\boldsymbol{k}(\boldsymbol{x}_3-\boldsymbol{x}'_3)} \\
&\quad\Bigg\langle(2\pi)^4\Bigg[\Bigg(\delta^{(2)}(\boldsymbol{x}_{13})\delta^{(2)}(\boldsymbol{x}_{1'3'})\sum_{h,g}\psi^{T,L}_{1;h,g}(\boldsymbol{x}_{12})\psi^{T,L,*}_{1';h,g}(\boldsymbol{x}_{1'2'}) + \{1,1'\}\leftrightarrow\{2,2'\}\Bigg) \\
&\qquad\cdot N^{(4)}(\boldsymbol{x}_1,\boldsymbol{x}'_1,\boldsymbol{x}'_2,\boldsymbol{x}_2) + \Bigg(\delta^{(2)}(\boldsymbol{x}_{23})\delta^{(2)}(\boldsymbol{x}_{1'3'})\sum_{h,g}\psi^{T,L}_{2;h,g}(\boldsymbol{x}_{12})\psi^{T,L,*}_{1';h,g}(\boldsymbol{x}_{1'2'}) \\
&\qquad\qquad + \{1,1'\}\leftrightarrow\{2,2'\}\Bigg)\cdot N^{(22)}(\boldsymbol{x}_1,\boldsymbol{x}'_1|\boldsymbol{x}'_2,\boldsymbol{x}_2)\Bigg] \\
&\quad + (2\pi)^2\Bigg[\delta^{(2)}(\boldsymbol{x}_{13})\sum_{h,g}\psi^{T,L}_{1;h,g}(\boldsymbol{x}_{12})\psi^{T,L,*}_{3';h,g}(\boldsymbol{x}_{1'3'},\boldsymbol{x}_{2'3'})N^{(24)}(\boldsymbol{x}_{3'},\boldsymbol{x}_{1'}|\boldsymbol{x}_{2'},\boldsymbol{x}_2,\boldsymbol{x}_1,\boldsymbol{x}_{3'}) \\
&\qquad + \{1\}\leftrightarrow\{2\} + \delta^{(2)}(\boldsymbol{x}_{1'3'})\sum_{h,g}\psi^{T,L}_{3;h,g}(\boldsymbol{x}_{13},\boldsymbol{x}_{23})\psi^{T,L,*}_{1';h,g}(\boldsymbol{x}_{1'2'}) \\
&\qquad\qquad\cdot N^{(24)}(\boldsymbol{x}_1,\boldsymbol{x}_3|\boldsymbol{x}_{2'},\boldsymbol{x}_2,\boldsymbol{x}_3,\boldsymbol{x}_{1'}) + \{1'\}\leftrightarrow\{2'\}\Bigg] \\
&\quad + \sum_{h,g}\psi^{T,L}_{3;h,g}(\boldsymbol{x}_{13},\boldsymbol{x}_{23})\psi^{T,L,*}_{3';h,g}(\boldsymbol{x}_{1'3'},\boldsymbol{x}_{2'3'})\cdot N^{(44)}(\boldsymbol{x}_1,\boldsymbol{x}_{1'},\boldsymbol{x}_{3'},\boldsymbol{x}_3|\boldsymbol{x}_3,\boldsymbol{x}_{3'},\boldsymbol{x}_{2'},\boldsymbol{x}_2)\Bigg\rangle_{A^+},
\end{aligned} \tag{10}$$

where $\psi_{i'} \equiv \psi_i$, $i = 1, \ldots, 3$ and $z_3 = 1 - z_1 - z_2$. To obtain sub-leading terms in N_c all operators $N^{(4)}, N^{(22)}, N^{(24)}, N^{(44)}$ are to be replaced by $1/N_c \cdot N^{(4)}(\boldsymbol{x}_1, \boldsymbol{x}_{1'}, \boldsymbol{x}_{2'}, \boldsymbol{x}_2)$. The super-scripts $T = \pm$ and L refer to transverse and longitudinal polarizations of the virtual photon while $h, g = \pm$ denote quark and gluon helicity respectively (due to helicity conservation in mass-less QCD the helicity of the anti-quark is always opposite to the quark helicity). To determine the wave functions ψ_i, $i = 1, \ldots, 3$ we factorize the color and Wilson-line structures from the amplitudes in Eq. (5) and evaluate Dirac and Lorentz structures using spinor helicity techniques [11], which provide a powerful alternative for the evaluation of scattering amplitude in the high energy limit; for details we refer to the paper in preparation [12]. With ϕ_{ij} the azimuthal angle of $\boldsymbol{x}_{ij}$, $i, j = 1 \ldots, 3$ and

$$X_j^2 = \boldsymbol{x}_{12}^2 (z_j + z_3)\,(1 - z_j - z_3)\,, \quad j = 1, 2, \qquad X_3^2 = z_1 z_2 \boldsymbol{x}_{12}^2 + z_1 z_3 \boldsymbol{x}_{13}^2 + z_2 z_3 \boldsymbol{x}_{23}^2\,, \tag{11}$$

we obtain

$$\begin{aligned}
\psi^L_{j,hg} &= \sqrt{2} Q K_0\,(Q X_j) \cdot a^{(L)}_{j,hg}, && j = 1, 2 \\
\psi^T_{j,hg} &= \frac{K_1\,(Q X_j)}{-i|\boldsymbol{x}_{12}| e^{\mp i \phi_{\boldsymbol{x}_{12}}}} \cdot a^{\pm}_{j,hg} && j = 1, 2 \\
\psi^L_{3,hg} &= 4\pi i Q \sqrt{2 z_1 z_2} K_0\,(Q X_3)\,(a^{(L)}_{3,hg} + a^{(L)}_{4,hg}), \\
\psi^T_{3,hg} &= 4\pi Q \sqrt{z_1 z_2} \frac{K_1\,(Q X_3)}{X_3} (a^{\pm}_{3,hg} + a^{\pm}_{4,hg})\,,
\end{aligned} \tag{12}$$

where the helicity amplitude $a^{(T,L)}_{k,hg}$ is directly extracted from the amplitude $i\mathcal{A}_k$, $k = 1, \ldots 4$. These helicity amplitudes satisfy the following relations,

$$a^{T,L}_{k+1,hg} = -a^{T,L}_{k,-hg}(\{p, \boldsymbol{x}_1\} \leftrightarrow \{q, \boldsymbol{x}_2\}), \qquad k = 1, 3\,, \quad a^{T,L}_{j,hg} = a^{(-T,L)*}_{j,-h-g}\,, \quad j = 1, \ldots, 4. \tag{13}$$

which allows to simplify the calculation using a minimal set of helicity amplitudes

$$\begin{aligned}
a^{(L)}_{1,++} &= -\frac{(z_1 z_2)^{3/2}\,(z_1 + z_3)}{z_3 e^{-i\theta_p}|\boldsymbol{p}| - z_1 e^{-i\theta_k}|\boldsymbol{k}|}, & a^{(L)}_{1,-+} &= -\frac{\sqrt{z_1} z_2^{3/2}\,(z_1 + z_3)^2}{z_3 e^{-i\theta_p}|\boldsymbol{p}| - z_1 e^{-i\theta_k}|\boldsymbol{k}|}, \\
a^{(L)}_{3,++} &= \frac{z_1 z_2}{|\boldsymbol{x}_{13}| e^{-i\phi_{\boldsymbol{x}_{13}}}}, & a^{(L)}_{3,-+} &= \frac{z_2(1 - z_2)}{|\boldsymbol{x}_{13}| e^{-i\phi_{\boldsymbol{x}_{13}}}}, \\
a^{(+)}_{1,++} &= -\frac{\sqrt{2}(z_1 z_2)^{3/2}}{z_3 e^{-i\theta_p}|\boldsymbol{p}| - z_1 e^{-i\theta_k}|\boldsymbol{k}|}, & a^{(+)}_{1,-+} &= \frac{\sqrt{z_1 z_2}(z_1 + z_3)^2}{z_3 e^{-i\theta_p}|\boldsymbol{p}| - z_1 e^{-i\theta_k}|\boldsymbol{k}|}, \\
a^{(+)}_{1,+-} &= -\frac{\sqrt{z_1} z_2^{3/2}(z_1 + z_3)}{z_3 e^{i\theta_p}|\boldsymbol{p}| - z_1 e^{i\theta_k}|\boldsymbol{k}|}, & a^{(+)}_{1,--} &= -\frac{z_1^{3/2}\sqrt{z_2}(z_1 + z_3)}{z_3 e^{i\theta_p}|\boldsymbol{p}| - z_1 e^{i\theta_k}|\boldsymbol{k}|}, \\
a^{(+)}_{3,++} &= \frac{z_1 z_2 (z_3 |\boldsymbol{x}_{23}| e^{-i\phi_{\boldsymbol{x}_{23}}} - z_1 |\boldsymbol{x}_{12}| e^{-i\phi_{\boldsymbol{x}_{12}}})}{(z_1 + z_3)|\boldsymbol{x}_{13}| e^{-i\phi_{\boldsymbol{x}_{13}}}}, \\
a^{(+)}_{3,+-} &= \frac{z_2 (z_3 |\boldsymbol{x}_{23}| e^{-i\phi_{\boldsymbol{x}_{23}}} - z_1 |\boldsymbol{x}_{12}| e^{-i\phi_{\boldsymbol{x}_{12}}})}{|\boldsymbol{x}_{13}| e^{i\phi_{\boldsymbol{x}_{13}}}}, \\
a^{(+)}_{3,-+} &= \frac{(z_1 + z_3)(z_3 |\boldsymbol{x}_{23}| e^{-i\phi_{\boldsymbol{x}_{23}}} - z_1 |\boldsymbol{x}_{12}| e^{-i\phi_{\boldsymbol{x}_{12}}})}{|\boldsymbol{x}_{13}| e^{-i\phi_{\boldsymbol{x}_{13}}}} \\
a^{(+)}_{3,--} &= \frac{z_1 (z_3 |\boldsymbol{x}_{23}| e^{-i\phi_{\boldsymbol{x}_{23}}} - z_1 |\boldsymbol{x}_{12}| e^{-i\phi_{\boldsymbol{x}_{12}}})}{|\boldsymbol{x}_{13}| e^{i\phi_{\boldsymbol{x}_{13}}}},
\end{aligned} \tag{14}$$

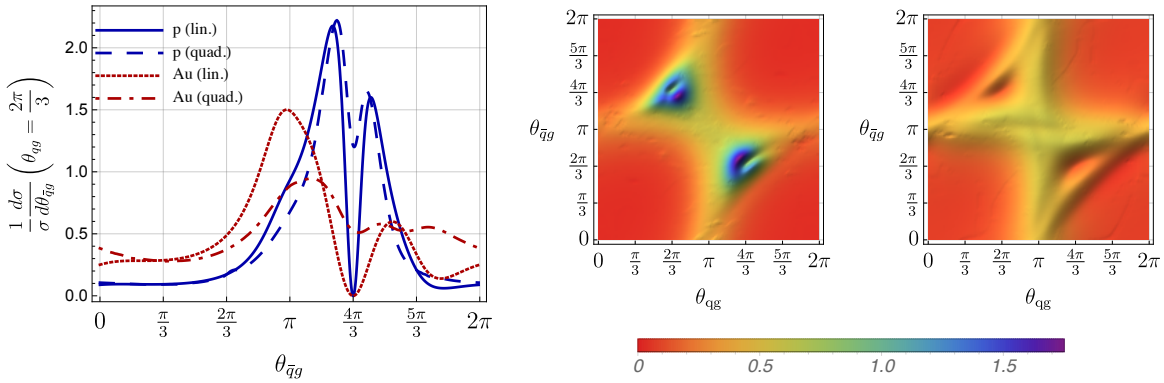

Figure 2: We fix $z_1 = z_2 = 0.2$, $|\boldsymbol{p}| = |\boldsymbol{k}| = |\boldsymbol{q}| = 2$ GeV and $Q = 3$ GeV. *Left:* Normalized cross-section against $\Delta\theta_{\bar{q}g}$ with $\Delta_{qg} = 2\pi/3$ for proton and gold up to linear and quadratic order in $N^{(2)}$. *Right:* Combined $\Delta\theta_{qg}$ and $\Delta\theta_{\bar{q}g}$ dependence of the normalized cross-section for proton and gold at quadratic order.

where $\theta_p, \theta_q, \theta_k$ denote the azimuthal angle of final state momenta and $|\boldsymbol{p}|, |\boldsymbol{q}|, |\boldsymbol{k}|$ their transverse momenta.

In absence of experimenally constrained quadrupole distributions we use for this first study the large N_c and Gaussian approximation to write the quadrupole $S^{(4)}$ in terms of the dipole $S^{(2)}$ [6]. Furthermore, we use a model of the dipole profile which is motivated by a fit to the solution of rcBK equation [4]

$$S^{(2)}_{(\boldsymbol{x}_1\boldsymbol{x}_2)} = \int d^2\boldsymbol{l}\, e^{-i\boldsymbol{l}\cdot\boldsymbol{x}_{12}}\, \Phi(\boldsymbol{l}^2) = 2\left(\frac{Q_0|\boldsymbol{x}_{12}|}{2}\right)^{\rho-1} \frac{K_{\rho-1}(Q_0|\boldsymbol{x}_{12}|)}{\Gamma(\rho-1)},$$
$$\text{where} \qquad \Phi(\boldsymbol{l}^2) = \frac{\rho-1}{Q_0^2\pi}\left(\frac{Q_0^2}{Q_0^2+\boldsymbol{l}^2}\right)^{\rho}, \tag{15}$$

and Q_0 is a scale proportional to the saturation scale. Since we are working in the dilute limit we study the cross-section at large photon virtuality $Q^2 = 9$ GeV^2 and expand Eq. (10) up to quadratic order in $N^{(2)} = 1 - S^{(2)}$. The free parameters are taken as $\rho = 2.3$ and $Q_0^{\text{proton}} = 0.69$ GeV which are motivated by inclusive DIS fits of the dipole distribution at $x = 0.2 \times 10^{-3}$. For the gold nucleus we use $Q_0^{\text{Au}} = A^{1/6} \cdot Q_0^{\text{proton}} = 1.67$ GeV. At the linear order in $N^{(2)}$, the cross-section is directly proportional to the Fourier transform of the dipole, $\Phi\left((\boldsymbol{p}+\boldsymbol{k}+\boldsymbol{q})^2\right)$ and therefore gives direct access to the gluon distribution in the target. In analogy to the back-to-back configuration in di-parton production we take $|\boldsymbol{p}| = |\boldsymbol{k}| = |\boldsymbol{q}|$. The 'collinear' limit $\boldsymbol{p}+\boldsymbol{k}+\boldsymbol{q} = 0$ of vanishing transverse momentum transfer between projectile and target corresponds then to the angular configuration $\{\Delta\theta_{qg}, \Delta\theta_{\bar{q}g}\} = \{2\pi/3, 4\pi/3\}$ and $\{\Delta\theta_{qg}, \Delta\theta_{\bar{q}g}\} = \{4\pi/3, 2\pi/3\}$, *i.e.* a Mercedes-Benz star configuration, which is characterized by strong peaks of the angular distribution at these points. We observe vanishing of the partonic cross section at these 'collinear' configurations, Fig. 2, accompanied by a strong double peak. This behavior is also observed in studies of quark-gluon, photon-quark and dilepton-quark angular correlations [13]. This vanishing of the partonic cross-section at these points is due to the vanishing of the partonic matrix element at leading order in $N^{(2)}$ for zero momentum transfer between projectile and target. Indeed such a behavior is expected

due to Ward identities applicable to the gluon exchange in the t-channel. This double peak will mostly go away at the hadronic level and/or when adding quadratic corrections in $N^{(2)}$, which already provides non-zero values at these points. The effect of a larger gluon saturation scale for a nucleus is clearly seen at the linear level in the figure. To explore the potential of the process to detect effects beyond the linear approximation, we further include sub-leading corrections in the dilute expansion. We find that these corrections are small in the case of the proton, while sizable for a highly saturated gold nucleus. This emphasizes the potential of the 3 parton production process in providing experimental evidence for saturation effects and in particular for exploring the 4-point correlator $S^{(4)}$. This is even more remarkable due to the rather large value of photon virtuality $Q^2 = 9$ GeV^2. A comprehensive numerical study of the three hadron/jet azimuthal angular correlations using the most up-to-date solutions of the rcBK equation will clearly help establish/constrain saturation dynamics against competing formalism such as collinear factorization, applicable to the low density regime. This is work in progress and will be reported elsewhere [12].

Acknowledgments

We would like to thank I. Balitsky, G. Beuf and Yu. Kovchegov for helpful discussions. We also would like to acknowldege use of the codes [14]. Support has been received in part by Consejo Nacional de Ciencia y Tecnología grant number 256494 and UNAM-DGAPA-PAPIIT grant number IN101515. M.H. acknowledges support by Consejo Naciona de Ciencia y Tecnología grant numbers CB-2014-22117 and CB-2014-241408 as well as the Red-FAE. J.J-M. acknowledges support by the DOE Office of Nuclear Physics through Grant No. DE-FG02-09ER41620 and from The City University of New York through the PSC-CUNY Research Award Program, grant 67732-0045. M.E.T.-Y. acknowledges support from Consejo Naciona de Ciencia y Tecnología sabbatical grant number 232946 and the kind hospitality of ICN-UNAM provided in the initial stages of this collaboration.

References

[1] L. V. Gribov, E. M. Levin and M. G. Ryskin, Phys. Rept. **100**, 1 (1983).

[2] L. D. McLerran and R. Venugopalan, Phys. Rev. D **49**, 2233 (1994), Phys. Rev. D **49**, 3352 (1994).

[3] E. Iancu and R. Venugopalan, In *Hwa, R.C. (ed.) et al.: Quark gluon plasma* 249-363; H. Weigert, Prog. Part. Nucl. Phys. **55**, 461 (2005); J. Jalilian-Marian, Y. V. Kovchegov, Prog. Part. Nucl. Phys. **56**, 104-231 (2006); F. Gelis, E. Iancu, J. Jalilian-Marian, R. Venugopalan, Ann. Rev. Nucl. Part. Sci. **60**, 463-489 (2010); J. L. Albacete and C. Marquet, Prog. Part. Nucl. Phys. **76**, 1 (2014).

[4] J. L. Albacete, N. Armesto, J. G. Milhano, P. Quiroga-Arias and C. A. Salgado, Eur. Phys. J. C **71**, 1705 (2011); A. H. Rezaeian, M. Siddikov, M. Van de Klundert and R. Venugopalan, Phys. Rev. D **87**, no. 3, 034002 (2013); A. H. Rezaeian and I. Schmidt, Phys. Rev. D **88**, 074016 (2013); E. Iancu, J. D. Madrigal, A. H. Mueller, G. Soyez and D. N. Triantafyllopoulos, Phys. Lett. B **750**, 643 (2015); J. L. Albacete, arXiv:1507.07120 [hep-ph].

[5] G. Beuf, Phys. Rev. D **85**, 034039 (2012); I. Balitsky and G. A. Chirilli, Phys. Rev. D **83**, 031502 (2011), Phys. Rev. D **87**, no. 1, 014013 (2013), R. Boussarie, A. V. Grabovsky, L. Szymanowski and S. Wallon, JHEP **1409**, 026 (2014).

[6] A. Kovner and U. A. Wiedemann, Phys. Rev. D **64**, 114002 (2001); J. Jalilian-Marian and Y. V. Kovchegov, Phys. Rev. D **70**, 114017 (2004) [Erratum-ibid. D **71**, 079901 (2005)]; A. Kovner and M. Lublinsky, JHEP **0611**, 083 (2006); F. Dominguez, C. Marquet, B. -W. Xiao and F. Yuan, Phys. Rev. D **83**, 105005 (2011).

[7] D. Kharzeev, E. Levin and L. McLerran, Nucl. Phys. A **748**, 627 (2005); C. Marquet, Nucl. Phys. A **796**, 41 (2007); J. L. Albacete and C. Marquet, Phys. Rev. Lett. **105**, 162301 (2010); T. Lappi and H. Mantysaari, Nucl. Phys. A **908**, 51 (2013).

[8] L. Zheng, E. C. Aschenauer, J. H. Lee and B. W. Xiao, Phys. Rev. D **89**, no. 7, 074037 (2014).

[9] J. C. Collins, Nucl. Phys. B **396**, 161 (1993) [hep-ph/9208213].

[10] Y. V. Kovchegov and H. Weigert, Nucl. Phys. A **784**, 188 (2007); I. Balitsky and G. A. Chirilli, Phys. Rev. D **77**, 014019 (2008); J. L. Albacete and Y. V. Kovchegov, Phys. Rev. D **75**, 125021 (2007).

[11] M. L. Mangano and S. J. Parke, Phys. Rept. **200**, 301 (1991); L. J. Dixon, In *Boulder 1995, QCD and beyond* 539-582 [hep-ph/9601359].

[12] A. Ayala, M. Hentschinski, J. Jalilian-Marian, M. E. Tejeda-Yeomans, in preparation.

[13] R. Baier, A. Kovner, M. Nardi and U. A. Wiedemann, Phys. Rev. D **72**, 094013 (2005); J. Jalilian-Marian and A. H. Rezaeian, Phys. Rev. D **86**, 034016 (2012); A. Stasto, B. W. Xiao and D. Zaslavsky, Phys. Rev. D **86**, 014009 (2012); A. H. Rezaeian, Phys. Rev. D **86**, 094016 (2012); E. Basso, V. P. Goncalves, J. Nemchik, R. Pasechnik and M. Sumbera, Phys. Rev. D **93**, no. 3, 034023 (2016).

[14] R. Mertig, M. Bohm and A. Denner, Comput. Phys. Commun. **64**, 345 (1991); V. Shtabovenko, R. Mertig and F. Orellana, arXiv:1601.01167 [hep-ph]; T. Hahn, Comput. Phys. Commun. **140**, 418 (2001); D. Binosi, J. Collins, C. Kaufhold and L. Theussl, Comput. Phys. Commun. **180**, 1709 (2009).